A New Calculation Model of Switched Reluctance Motor for Use on Spice

O. Ichinokura, *Member, IEEE*, S. Suyama, T. Watanabe, *Member, IEEE*, and H. J. Guo, *Member, IEEE*

***Abstract*—This paper presents a new calculation model of the switched reluctance motor (SRM) for use on SPICE which is a general-purpose circuit simulation program. In the calculation model, the electric circuit and magnetic circuit of SRM are separated and are coupled by proper controlled sources. Using the SPICE model, we can calculate readily and accurately the dynamic characteristics of the SRM.**

***Index Terms*—Dynamic characteristics, numerical analysis, SPICE, SRM.**

I. Introduction

THE SWITCHED reluctance motor (SRM) exhibits desirable features including simple construction, high reliability and low cost. However, SRM was confined to special uses such as fuel pump because of its torque ripple and acoustic noise.

In recent years, the disadvantages of SRM have been improved by development of power electronics circuit technology [1]–[5]. Now, SRM is employed for the electric washing machine and electric bicycle. It is expected that SRM will have a growing application in the future.

Several papers have reported on the analysis of the SRM [6]–[10]. Most of the papers present static characteristics such as static-torque based on a FEM analysis. Few papers have reported quantitative analysis of dynamic characteristics of the SRM. So, the optimum design of the SRM have not been clarified fully.

In the previous paper [11], the authors proposed an analysis of SRM based on the general-purpose circuit simulation program "SPICE." The calculated results qualitatively agree with the experimental ones. For optimum design, however, it is necessary to improve the preciseness of the calculated values. In this paper, the authors present a new calculation model of SRM.

II. Fundamental Operation

Fig. 1 shows a schematic diagram of the SRM used in this paper. The pole number of the stator and rotor are 8 and 6, respectively. The core material is nonoriented silicon steel with a thickness of 0.5 mm. Fig. 2 is the driving circuit of the SRM. A four-phase transistor converter is used for the circuit.

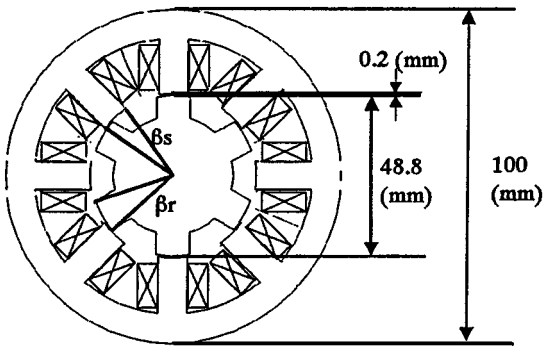

Stator pole arc βs	20.1 deg.
Rotor pole arc βr	23.5 deg.
Stack length	50 mm
Number of turns in the windings(per pole)	52 turns

Fig. 1. Schematic diagram of the SRM used in this paper.

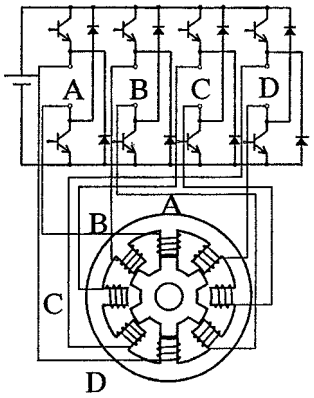

Fig. 2. Configuration of the driving circuit.

Now, let the rotor position be θ, which is 0° when the rotor is in the aligned position relative to the phase A stator pole as shown in Fig. 2. The winding inductance of the phase A is maximum at $\theta = 0°$, and is minimum at $\theta = 30°$. The torque is given by the inductance and exciting current as:

$$\tau = \frac{1}{2} i^2 \frac{dL(\theta)}{d\theta}. \tag{1}$$

In order to obtain the relationship between the inductance and rotor position, we calculate the magnetization curves for various

Manuscript received October 13, 2000.

O. Ichinokura is with the Department of Electrical and Communication Engineering, Tohoku University, Sendai 980-8597, Japan (e-mail: ichinoku@ecei.tohoku.ac.jp).

S. Suyama was with the Department of Electrical and Communication Engineering, Tohoku University. He is now with Hyogo works, Kawasaki Heavy Industries Ltd., Kobe 652-0884, Japan.

T. Watanabe and H. J. Guo are with the Department of Electrical and Communication Engineering, Tohoku University, Sendai 980-8597, Japan.

Publisher Item Identifier S 0018-9464(01)07089-3.

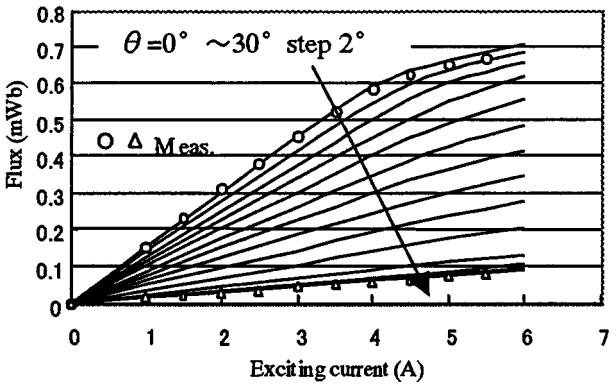

Fig. 3. Magnetization curves for various rotor positions.

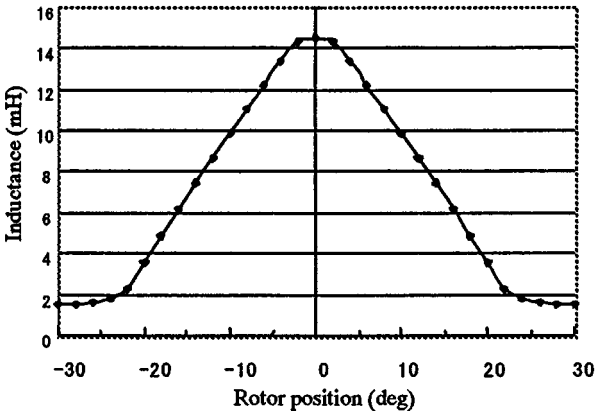

Fig. 4. Inductance versus rotor position curve.

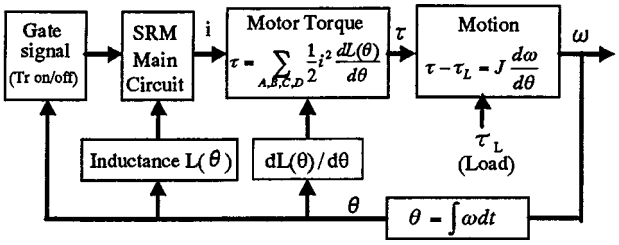

Fig. 5. Flow diagram of the calculations.

rotor positions using FEM analysis. Fig. 3 shows the magnetization curves calculated in the phase A pole. The measured values at $\theta = 0°$ and 30° are plotted in the figure. Although the magnetization curves have nonlinearity when the flux increases, we obtain the inductance from the magnetization curves by approximating a straight line in order to simplify the calculations.

Fig. 4 shows the relationship between the inductance and rotor position. The curves can be expressed with fourier series. Then we can analyze the operation of SRM based on the circuit and motion equations. In the next section, we carry out the calculation utilizing a general- purpose circuit simulation program "SPICE."

III. Calculation Method and Results

Fig. 5 shows a flow diagram of the calculation. When the rotor position θ is given, a gate signal of the transistor of the driving circuit is determined, and the exciting currents of the

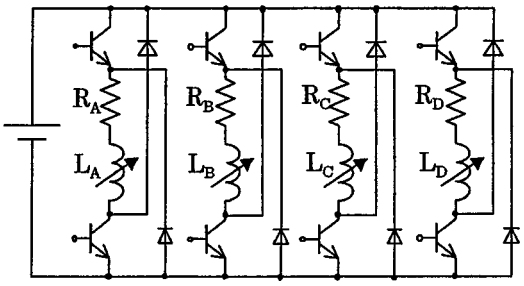

Fig. 6. Main circuit of SRM.

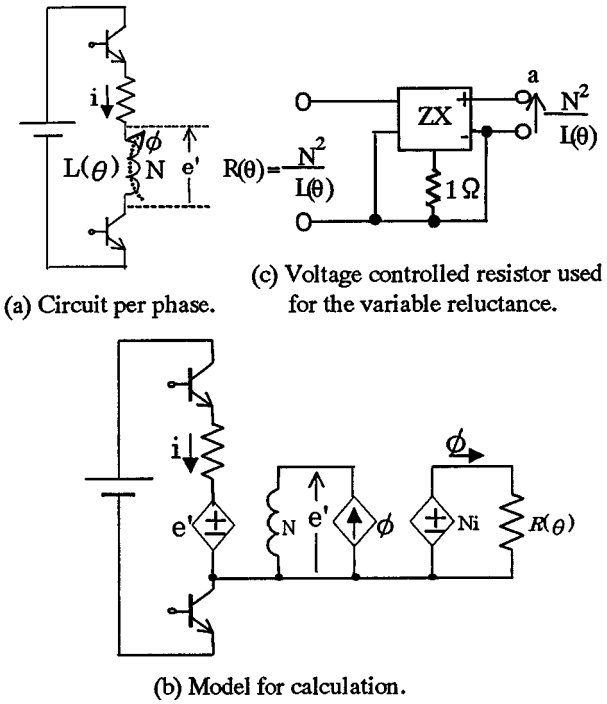

Fig. 7. Calculation model of SRM constructed with the electric and magnetic circuits.

SRM are calculated in the main circuit. From the currents and differential of the inductance $dL(\theta)/d\theta$, we obtain the motor torque τ. When the load torque τ_L is given, we can obtain the angular velocity ω based on motion equation. The integral of ω gives the rotor position θ.

In the SPICE simulation, above calculations are carried out by the equivalent circuit [11]. Fig. 6 shows the SRM main circuit. In the figure, R_A, R_B, R_C and R_D are resistance of the windings of the phase A, B, C and D, respectively. L_A, L_B, L_C and L_D are inductance of the windings, and change with the rotor position in the same manner as shown in Fig. 4. In the previous paper [11], we used a voltage-controlled inductor, which is additional component to PSPICE [12], as the variable inductance. The simulation results qualitatively agree with the experimental ones. But the quantitative difference between them cannot be disregarded. One reason is that the voltage-controlled inductor seems to be not sufficient for expressing the speed induced voltage due to the dynamically changing variable inductance. In this paper, we present a calculation model in which the electric and magnetic circuits are separated as shown in Fig. 7.

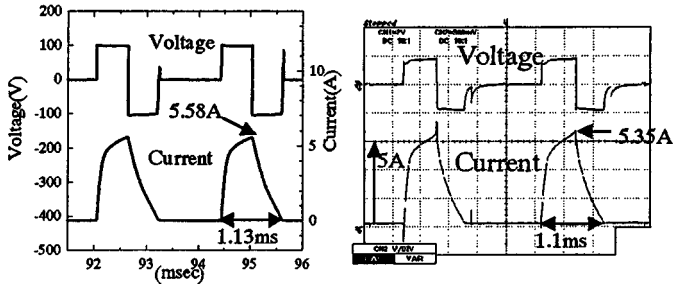

Fig. 8. Comparison between the calculated waveforms and measured ones.

In Fig. 7(a), i, ϕ and e' are the exciting current, flux and induced voltage, respectively. N is the number of turns in the exciting winding. Now, let the magnetic reluctance be $R(\theta)$. That is,

$$R(\theta) = \frac{N^2}{L(\theta).} \tag{2}$$

The relation between MMF and flux is

$$Ni = R(\theta)\phi. \tag{3}$$

The induced voltage e' is given by

$$e' = N\frac{d\phi}{dt.} \tag{4}$$

In Fig. 7(b), the right circuit expresses the (3). Ni is a voltage source controlled by the exciting current i. Using the calculated flux ϕ, the induced voltage e' is given by the center circuit. The value of the inductance is $N[H]$ which is equal to the number of turns in windings. In the left circuit, e' is the voltage controlled voltage source. As the variable reluctance, we can use a voltage controlled-resistor as shown in Fig. 7(c).

Based on the calculation model, we compute the operating characteristics of the SRM. Fig. 8 shows the comparison between the calculated waveforms and measured ones. It reveals that the calculated values and measured ones show a good agreement.

Fig. 9 shows the torque versus speed characteristics obtained for various values of input dc voltage V_d. The dashed curves show the calculated values and the solid curves the measured ones. This reveals that the calculated values agree well with the measured ones.

IV. Conclusion

We propose a new calculation model of SRM for use on SPICE. The calculated results and measured ones show a good agreement. The analytical method developed here is useful for optimum design of SRM because we can calculate readily and accurately the dynamic characteristics of SRM by the method.

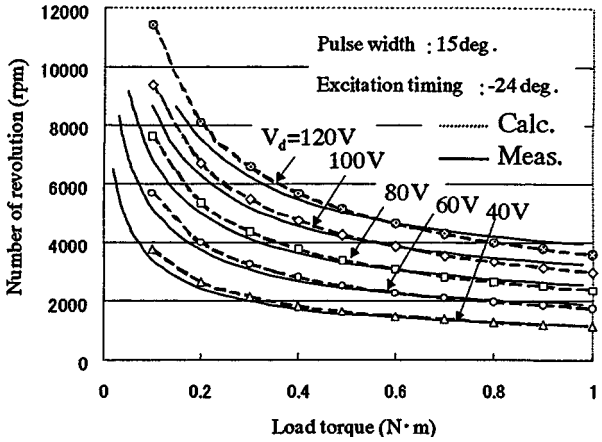

Fig. 9. Torque versus speed characteristics.

References

[1] P. J. Lawrenson, J. M. Stephanson, P. T. Blebkinsop, J. Corda, and N. N. Fulton, "Variable-speed switched reluctance motors," *IEE Proc.*, pt. B, vol. 127, pp. 253–265, 1980.

[2] W. Ray, P. J. Lawrenson, R. M. Davice, J. M. Stephanson, N. N. Fultonand, and R. J. Blake, "High-performance switched reluctance brushless drives," *IEEE Trans. Ind. Applicat.*, vol. IA-22, pp. 722–730, 1986.

[3] R. C. Becerra, M. Ehsani, and T. J. E. Miller, "Commutation of SR motors," *IEEE Trans. Power Electron.*, vol. 8, pp. 257–263, 1993.

[4] T. A. Lipo and Y. Li, "The CFM—A new family of electrical machines," in *Proceedings of IPEC-Yokohama '95*, 1995, pp. 1–9.

[5] C. A. Ferreira, S. R. Jones, B. T. Drager, and W. S. Heglund, "Design and implementation of a five-hp, switched reluctance, fuel-lube, pump motor drive for a gas turbine engine," *IEEE Trans. Power Elect.*, vol. 10, pp. 55–61, 1995.

[6] A. V. Radun, "Design considerations for the switched reluctance motor," *IEEE Trans. Ind. Applicat.*, vol. 31, pp. 1079–1087, 1995.

[7] A. Rudun, "Analytical calculation of the switched reluctance motor's unaligned inductance," *IEEE Trans. Magn.*, vol. 35, pp. 4473–4481, 1999.

[8] H. B. Ertan, "Prediction of and inductance displacement characteristics of asymmetrically slotted variable-reluctance motors using a simplified model for numerical field solution," *IEEE Trans. Magn.*, vol. 35, pp. 4247–4258, 1999.

[9] N. M. Abe, J. R. Cardoso, and L. Gualberto, "A virtual lab for electric motors and drives," *IEEE Trans. Magn.*, vol. 35, pp. 1674–1677, 1999.

[10] D. A. Staton, M. I. McGilp, T. J. E. Miller, and G. Gray, "High-speed PC-based CAD for motor drives," in *IEE Conf. Publ. (Inst. Electr. Eng.) (GBR)*, vol. 6, pp. 26–31.

[11] O. Ichinokura, T. Onda, M. Kimura, T. Watanabe, T. Yanada, and H. J. Guo, "Analysis of dynamic characteristics of switched reluctance motor based on SPICE," *IEEE Trans. Magn.*, vol. 34, pp. 2147–2149, 1998.

[12] P. W. Tuinenga, *SPICE—Guide to Circuit Simulation & Analysis Using Pspice*: Prentice Hall, 1988, pp. 189–191.